

# Adaptive Geolocation Based Interference Control for Hierarchical Cellular Network with Femtocells

Shweta Sagari, Gautam Bhanage, Dipankar Raychaudhuri  
 {shsagari, gautamb, ray}@winlab.rutgers.edu  
 WINLAB, Rutgers University, North Brunswick, NJ 08902, USA.

**Abstract**—This paper presents an adaptive interference control method to mitigate undesirable interference from femtocells to macrocell users in hierarchical cellular networks. Such mechanisms usually require over-the-air signalling for estimation of interference resulting significant bandwidth overhead. The proposed ‘Adaptive Interference Scaling’ (AIS) method uses geolocation information for femtocell power control for interference avoidance. In this approach, each femtocell calculates interference contributed to nearby macrocell users and adjusts the power to meet specific target signal-to-interference-plus-noise (SINR) level. Results from simulations show that AIS is able to increase the number of macrocell users achieving target data rates by up to 158% relative to baseline without adaptive control, while resulting in only 12.2% femtocell users receiving rates below the target. AIS achieves improved performance by using location information to calculate and limit the interference power contributed by femtocells to macrocell users, while allowing the network operator to set any desired target rates.

**Index Terms**—femtocell, macrocell, interference mitigation, CDMA, cellular system evaluation

## I. INTRODUCTION

Femtocells improve cellular coverage in SOHO (Small Office, Home Office) environments with connection to cellular operator’s core network using an IP based backhaul [1]. 3G/CDMA femtocells are already being deployed by operators and mobile manufacturers [2], [3]. Co-channel operation of such femtocells with existing macro-cellular networks can significantly improve the spectral efficiency in comparison with dedicated channels assignment to each macrocell and femtocell users [4], [5], [6]. In such deployments, open access femtocells allows cellular users to connect to near-by base-station (macro or femto base-station) with the best signal quality but at the expense of increased handovers between base-stations [7], [8]. A closed access femtocell, on the other hand, is accessible to only registered users which ensures privacy, and has the advantage of constant high signal-to-noise ratio and data rate. However, closed access femtocells can pose serious interference to near-by macrocell users, thus degrading the performance of the macrocell [9], [6]. Our work studies achievable performance of interference mitigation schemes in a co-channel deployment of closed access femtocells, primarily in downlink scenarios.

### A. Motivation and Problem Definition

In most previous studies, the system infrastructure needs to exchange information (e.g. channel gain, load spillage,

measurement reports etc.) between the macrocell and the femtocell to coordinate interference management between them. In a typical approach, measurement of channel gain is done through explicit beaconing. For example, Rangan et. al [10] use an implementation of signal beaconing to calculate the channel gain between the femtocell and the macrocell user (MUE). This scheme requires the MUE to transmit a reference signal intermittently on the uplink and the femtocells to stop their normal reception. Although such mechanisms are able to effectively mitigate interference for the MUEs, they impose the following additional requirements on the system: (1) Explicit channel for signalling and interference estimation, and (2) synchronization across femtocells and MUEs.

An important aspect in this explicit signaling and interference estimation mechanism is that the overheads grow in direct proportion to the density of the femtocell users. For example, consider a 3G CDMA based system. In this case, if beacon messages (for estimation) are broadcasted by MUE to surrounding femtocells at the control data rate of 38.4kbps, the channel is occupied for a minimum time period of 26.66ms per femtocell base-station. These overheads can lead to a loss of up to 18Mbps of bandwidth with a femtocell deployment that has up to 30% overlap with the macrocell coverage.

The above mentioned overheads can be saved if information exchange and estimation over-the-air can be avoided. Hence, we propose the AIS interference mitigation scheme which takes advantage of location information and the IP backhauling for interference mitigation. Specifically, the contributions of our study are:

- 1) Interference Characterization: We begin by showing that there is significant deterioration in performance due to co-channel interference across macrocells and femtocell.
- 2) AIS Mitigation: We propose the Adaptive Interference Scaling (AIS) mechanism that implements power control across macrocell-femtocell networks purely based on interference estimation using geolocation information.
- 3) System Evaluation: System performance evaluations show that (1) the scheme is able to allow programmable interference control, and (2) it performs well even under the absence of accurate location information.

**Paper organization:** The rest of the paper is organized as follows. Section II will provide a brief discussion on the related work. Section III presents the network and interference models used in our study. The AIS interference mitigation

TABLE I  
NOTATIONS AND DEFINITIONS USED THROUGHOUT THE PAPER

Signal-to-interference plus noise ratio (SINR)	$\gamma$
Macrocell base-station	MBS
Femtocell base-station	FBS
Macrocell user	MUE
Femtocell user	FUE
Femto density	$\eta$
Wall loss	$L_w$
Transmission power of MBS(m) or FBS(f) x	$\Phi^x$
Channel gain between base-station x and user y	$h_{x,y}$
Interference from base-station x to user y	$I_{x,y}$
Outage probability	$\psi$

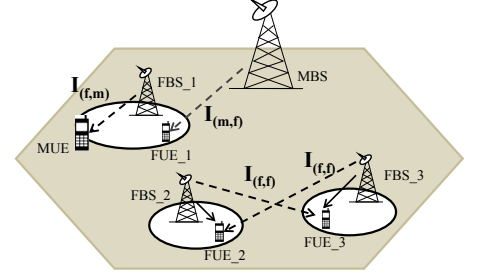


Fig. 1. Downlink interference scenarios in coexistent operation of macrocell and femtocell users.

algorithm is discussed in Section IV. System evaluations are presented in Section V. Finally, Section VI discusses the conclusions and future directions.

## II. RELATED WORK

Interference management/coordination in coexistent scenarios of macrocell and femtocell is well studied problem and several approaches have been proposed. References [7] and [8] consider the femtocell power configuration based on received power from the macrocell base-station. This solution works well in case of open-access, low density femtocells with large wall separation. References [11] and [10] offer power control solutions based on the utility maximization in cellular system based on non-cooperative game theory and load-spillage algorithm respectively. Reference [11] also proposes concept of reducing power of femtocells which are in near-by region of the MBS in uplink. Reference [12] encounters interference mitigation with usage of frequency division duplexing (FDD) in WCDMA with carrier separation. We consider though whole CDMA spectrum to increase spectrum utilization [4]. Reference [13] provides interference analysis for OFDMA system by utilizing resource blocks of MUEs which are away the femtocell through spectrum sensing and MUE scheduling information. Reference [5] also studies interference avoidance in OFDMA through scheduling of sub-carriers by spectrum sensing and measurement reports given by femtocell users. As opposed to explicit interference measurements used in all the previous work, our approach exploits geolocation information available at macrocell users and base-stations for interference estimation and mitigation.

## III. SYSTEM SETUP

### A. Network Setup

Table (I) summarizes the notations which will be used in the rest of this paper. Our setup consists of a 3G/CDMA 1xEV-DO network analyzed for downlink, considering variable data rate availability at both macrocell and femtocell [14]. We assume a hexagonal macrocell structure of 19 adjacent cells, while evaluating the central cell  $C_0$  with a macro base-station  $B_0$ . Macrocell users (MUE) and femtocells are uniformly randomly distributed in  $C_0$  with number  $M$  and  $F$  respectively. Each MUE $_i \forall i \in \{1, 2, \dots, M\}$ , is associated with  $B_0$ . Let's assume that only one femtocell user FUE $_j$  is associated

TABLE II  
CHANNEL MODELS SUGGESTED BY 3GPP [15]

Path Loss	
MBS to MUE	$15.3 + 37.6\log(R)$
FBS to FUE (both belong to same femto)	$38.46 + 20\log(R) + 0.7R$
FBS to FUE (both belong to different femtos)	$15.3 + 37.6\log(R) + L_w$
FBS to MUE	$15.3 + 37.6\log(R) + L_w$
Log-Normal Shadowing	
Outdoor	$Std.dev = 8.9dB$
Indoor	$Std.dev = 4dB$

with each FBS $_j, j \in \{1, 2, \dots, F\}$ . Let  $\eta$  be the density of femtocells corresponding to the percentage of area overlapped between the macrocell and femtocell. Wall loss corresponding to each femtocell is chosen with equiprobability from a given set of values [8], [7]. No relative motion is considered between any base-station and user. Channel is modeled considering path-loss and log-normal shadowing as given in Table (II).

### B. Interference Model

We use notations  $i \in \{1, 2, \dots, M\}$  and  $j \in \{1, 2, \dots, F\}$  for MUE and FUE respectively. We also use notations  $p \in \{0, 1, 2, \dots, 18\}$  and  $q \in \{1, 2, \dots, F\}$  for MBS and FBS respectively where  $p = 0$  represents  $B_0$ . Assume  $\Phi_p^m$  and  $\Phi_q^f$  as the transmitter power of MBS and FBS respectively. We define the downlink interference scenarios described in Figure 1 as:

**Interference to MUE $_i$ :** The *co-layer interference* from adjacent MBSs is given as:  $I_{m,m} = \sum_{p \neq 0} \Phi_p^m h_{pi}$ . The *cross-layer interference* from near-by FBSs which act as dominant sources of interference to each MUE is given as:  $I_{f,m} = \sum_q \Phi_q^f h_{qi}$ .

**Interference to FUE $_j$ :** The *co-layer interference* from adjacent FBSs which acts as a dominant source of interference to FUEs is given as:  $I_{f,f} = \sum_{q \neq j} \Phi_q^f h_{qj}$ . The *cross-layer interference* from the nearest MBS i.e.  $B_0$  is given as:  $I_{m,f} = \Phi_0^m h_{pj}$ .

## IV. ADAPTIVE INTERFERENCE SCALING

We propose the Adaptive Interference Scaling (AIS) based power adjustment scheme to mitigate femtocell interference to near-by MUEs. It is based on estimation and adaptive scaling of dominant interference contributed by each femtocell. This

scheme avoids interference estimation over-the-air by using approximate geo-location information available in the system<sup>1</sup>. Accordingly, power adjustment is initiated at MBS  $B_0$  using communication of information/control messages through backhaul. The network operator can control the frequency of use of our scheme depending on network mobility and its policies.

Let us make some assumptions which are applicable to AIS: (1) The interference range of each FBS is defined at some constant value  $D_I$  meters. (2) Every FBS provides location information using GPS capability<sup>2</sup>. Location information of the MUE can be obtained through triangulation, and the errors in triangulation are low, and (3) Channel conditions will remain same throughout one iteration of algorithm.

The AIS scheme is implemented in two sequential stages that are run iteratively at the MBS:

### A. Stage 1: Femtocell Power Rate Adaptation

We apply modified Foschini-Miljanic (FM) algorithm [16] to adjust femtocell power according to SINR corresponding to the required data rate. Consider  $\gamma_j$  and  $\Gamma_j$  to be the received and target SINR of the FUE <sub>$j$</sub>  which is connected to the FBS <sub>$j$</sub>  with transmission power  $\Phi_j^f$ , where  $j \in \{1, 2, \dots, F\}$ , and  $\gamma_j \neq \Gamma_j$ . Then, according to the FM algorithm, revised power of FBS <sub>$j$</sub>  is given as:  $(\Phi_j^f)_0 = \min(\Phi_j^f \cdot \frac{\Gamma_j}{\gamma_j}, \Phi_{max}^f)$ . Where,  $\Phi_{max}^f$  is the maximum power constraint for the FBS. As this function adjusts the power of FBS <sub>$j$</sub>  according to the needs of the FUE <sub>$j$</sub> , thus, minimizes interference. In addition, we take a heuristic approach in *stage 2* to mitigate interference from FBSs to MUEs.

### B. Stage 2: Femto-macro Interference Mitigation

The second stage of the AIS scheme adjusts the transmission power of every FBS ( $\Phi^f$ ) which lies in the proximity of a MUE. It chooses the dominant FBS interferers for every MUE and assigns weights/reduction factors in proportion to the interference they are causing. The AIS scheme uses FBS information such as unique FBS ids,  $\Phi^f$ s and geo-location coordinates at the MBS  $B_0$ <sup>3</sup> which can be passed from femtocells through the backhaul. Using this information interference estimation for the MUE is followed by power adjustment at FBSs, which is done as discussed below.

Let us consider a MUE <sub>$i$</sub> , where  $i \in \{1, 2, \dots, M\}$ , where received SINR is given by,

$$\gamma_i = \frac{\Phi^m h_{0i}}{I_{m,m} + I_{f,m} + N_0} \quad (1)$$

where,  $N_0$  is the noise in an additive white gaussian noise (AWGN) channel. We also define  $\gamma_i^*$  which denotes the target SINR. If  $\gamma_i < \gamma_i^*$ , then MUE <sub>$i$</sub>  is assumed to be at poor

<sup>1</sup>Position of every FBS is known because they are equipped with GPSs which are currently used only for synchronization. Approximate position of the MUE is known through triangulation.

<sup>2</sup>A GPS is available by default on all basestations for synchronization, and can be used to further obtain location information.

<sup>3</sup>Power control using AIS is implemented at FBSs in correspondence to the nearest MBS  $B_0$ .

signal quality, and  $B_0$  initiates power adjustment of FBSs, in proximity of MUE <sub>$i$</sub> .

Let us consider  $S_{Fi}$  as the set of  $l$  FBSs around the MUE <sub>$i$</sub>  in radius  $D_I$ . Further  $F_q \in S_{Fi}$ , where  $q \in \{1, 2, \dots, l\}$ , each  $F_q$  contributes to interference in  $I_{f,m}$ . Assuming  $I_{f,m}$  as dominant interference to MUE <sub>$i$</sub> , ( $I_{m,m} + N_0 \ll I_{f,m}$ ), we ignore  $I_{m,m} + N_0$  from Eq. (1) as,

$$\gamma_i = \frac{\Phi^m h_{0i}}{I_{f,m}} = \frac{\Phi^m h_{0i}}{\sum_q \Phi_q^f h_{qi}} \quad (2)$$

where,  $\Phi_q^f$  is current transmission power of  $F_q$ . At  $B_0$ , the channel gain  $h_{qi}$  is calculated using a static pathloss model with distance measurements obtained from geolocation coordinates. This model depends on the terrain around  $B_0$ . We define the target SINR margin for MUE <sub>$i$</sub>  as,  $\Delta_i = \frac{\gamma_i^*}{\gamma_i}$ . Assuming constant received power at MUE <sub>$i$</sub>  from  $B_0$  with reference to Eq. (2), we get,

$$\Delta_i = \frac{(\sum_q \Phi_q^f h_{qi})_c}{(\sum_q \Phi_q^f h_{qi})_t} = \frac{\sum_q \Phi_q^f h_{qi}}{\sum_q (\Phi_q^f)^* h_{qi}} \quad (3)$$

where suffix  $c$  and  $t$  represents for current and target values.  $(\Phi_q^f)^*$  represents transmission power of  $F_q$  after power adjustment to achieve target SINR margin.

Let us define contribution of interference by each  $F_q$  in current  $I_{f,m}$  by factor  $k_q$ , such that,

$$\Phi_q^f h_{qi} = k_q (\sum_q \Phi_q^f h_{qi}) \quad (4)$$

where,  $\sum_q k_q = 1$ . We consider  $w_q$  as the scaling factor applied to  $\Phi_q^f$  to achieve desired transmit power as,

$$(\Phi_q^f)^* = w_q \Phi_q^f \quad (5)$$

Hence, from Eq. (3), Eq. (5) and Eq. (4), we have the relation,

$$\Delta_i = \frac{\sum_q \Phi_q^f h_{qi}}{\sum_q w_q k_q (\sum_q \Phi_q^f h_{qi})} = \frac{1}{\sum_q w_q k_q} \quad (6)$$

Thus, larger the contribution of interference from  $F_q$  (large  $k_q$ ) to MUE <sub>$i$</sub> , AIS does a larger reduction in  $\Phi_q^f$ , and corresponding smaller should be the  $w_q$ . Considering a linear relationship between  $k_q$  and  $w_q$  we get,

$$k_q \propto \frac{1}{w_q} \Rightarrow k_1 w_1 = k_2 w_2 = \dots = k_l w_l = \text{constant} \quad (7)$$

Thus, solving Eq. (6) using Eq. (7) for  $w_q$ , we get,

$$w_q = (l \cdot k_q \cdot \Delta_i)^{-1} \quad (8)$$

AIS will use Eq. (5) and Eq. (8), to adjust the transmission power of  $F_q$ . To compensate for any estimation errors, the AIS scheme operates in an iterative correction mode in which, after the power adjustment at  $F_q$ ,  $B_0$  checks SINR gain at MUE <sub>$i$</sub> . Depending on the SINR gain, algorithm resets the target SINR margin of MUE <sub>$i$</sub>  and recalculates the  $(\Phi_q^f)^*$  value. This correction is repeated until it achieves the target SINR at MUE <sub>$i$</sub> . In a scenario where a FBS is dominant interferer to more than one MUE, this algorithm set minimum of transmission power required by each MUE.

TABLE III  
SIMULATION PARAMETERS BASED ON 3GPP

PARAMETER	VALUE
Operating Frequency	2 GHz
Bandwidth	1.25 MHz
Data Rate Availability	38.4 to 2457.6 kbps
SINR requirement	-12 to 9.7 dB
<b>Macrocell Parameters</b>	
Number of Macrocell Users ( $N_m$ )	20/km <sup>2</sup>
Inter-Site Distance (ISD)	2 km
MBS Transmission Power ( $\Phi_m^t$ )	42 dBm
<b>Femtocell Parameters:</b>	
femto density ( $\eta$ )	5% to 20%
Maximum Transmission Power ( $(\Phi_f^t)_{max}$ )	125 mW
Target Range	20 m
Wall Loss ( $L_w$ ) for glass, door and light internal/ /internal/external walls resp.	[1, 3, 7, 10, 15] dB
Simulation Iterations	1000

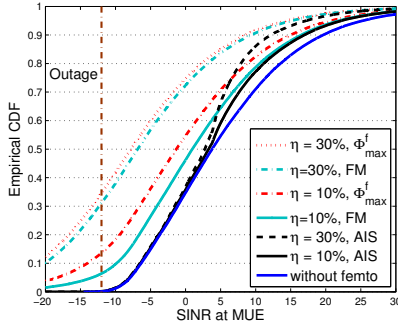


Fig. 2. Performance of the CDF of SINRs for MUEs based on proposed schemes when femto density = 10% and 30%

## V. EVALUATION

Performance of MUEs based on AIS is compared with the following cases: (1) When no femtocell is present which signifies the ideal case for MUEs with no femto interference. (2) when FBS power is set at maximum ( $\Phi_{max}^f$ ), and finally, (3) when FBS power is set based on FM. Performance of FUEs based on AIS is compared with cases when FBS power is set: at maximum ( $\Phi_{max}^f$ ), and based on FM. Important simulation parameters are given in Table (III).

### A. SINR Performance

We compare the SINR distribution achieved in relation to the scenarios mentioned above. For both MUEs and FUEs, we assume that the minimum required satisfactory data rate ( $R_g$ ) is 1200Kbps. We plot these results for two different femto densities ( $\eta$ ) 10% and 30%<sup>4</sup>.

Figure 2 shows CDF of SINR values for the MUEs. Best MUE performance is achieved in the ideal case. Worst case performance is achieved at the maximum value of FBS transmit power  $\Phi_{max}^f$ . At lower femto densities, FM does well, but it is unable to provide significant interference reduction for

<sup>4</sup>Femto density 10% is the average expected femtocell penetration in sub-urban areas. 30% is close to upper bound of femto density of any deployment

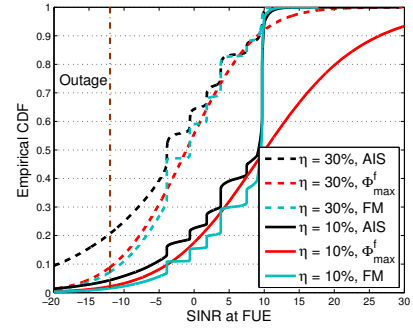


Fig. 3. Performance of the CDF of SINRs for FUEs based on proposed schemes when femto density = 10% and 30%

$\eta = 30\%$ . AIS achieves MUE SINRs close to the ideal case for both values of  $\eta$ . AIS allows the network provider to decide and deploy the femtocells with MUE target SINR provisioned based on its service level agreements (SLA). Once the target SINR for the MUEs is achieved, AIS does not reduce any further power for the FBSs surrounding the MUE. Due to this feature we see that AIS matches the ideal case up to the target SINR (which is set to 3.8dB in this case), and then gives a preference to FUEs. At best, we observe that AIS is able to increase the number of MUEs achieving target data rate by over 158% over those supported by  $\Phi_{max}^f$ .

Figure 3 shows the CDF of SINR values for FUEs. FM achieves the best FUE performance among all cases for both values of  $\eta$ , since it only tries to reduce inter-femto interference. Since AIS reduces FBS powers to improve SINR for MUEs, SINR values of FUEs are consequently lesser. Performance of the FUEs is worse because of our system design parameter of providing a target SINR of 3.8dB for MUEs. If this target is lowered, performance of the FUEs would improve significantly. Similar performance trends are seen for  $\eta = 30\%$ . However, due to increased density, AIS reduces power of more FBSs to achieve target MUE SINRs. We observe that AIS results in up to 12.2% of users not being able to achieve the target rates as compared to those supported by  $\Phi_{max}^f$ .

### B. Outage Probability

We now determine the outage performance of the AIS scheme for varying levels of femtocell deployment densities ( $\eta$ ). It is desired that the outage probability  $\psi$  of MUEs be 0.002. Figure 4 plots the outage probabilities for both MUEs and FUEs. In case of MUEs, AIS maintains  $\psi$  values in the range of 0.002 to 0.004, which are close to the ideal case. Thus, it is seen that MUE performance for AIS is robust even in case of addition of femtocells in network or change in femtocell topology. On the other hand, as  $\eta$  increases  $\psi$  of MUEs increases both for FM and  $\Phi_{max}^f$ . In the worst case it is seen that  $\Phi_{max}^f$  can result in an outage probability of 35%. In case of FUEs, as in the earlier case, FM has the best performance with  $\psi$  values ranging from 0.006 to 0.072

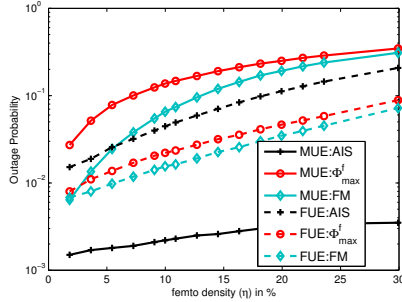


Fig. 4. Outage probability of MUEs and FUEs with respect to varied femto density ( $\eta$ ) based on proposed schemes

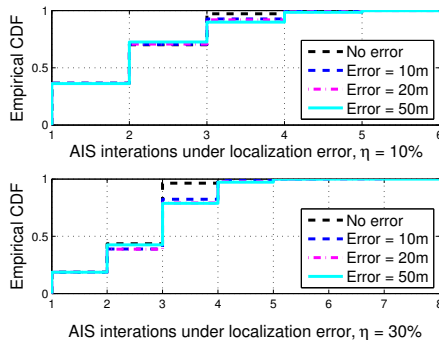


Fig. 5. Distribution of AIS convergence for femto densities at 10% and 30%

over a given range of  $\eta$ . As expected AIS reduces FBS power resulting in a worst case performance of up to 20% FUEs in outage.

### C. Localization Error

An important contribution of the AIS interference mitigation mechanism is the reduction in system overheads for interference estimation through the use of location information. However, in case of errors in location estimation, the performance of such a system could deteriorate. In this experiment, we describe the number of additional iterations (corrections) that would be required by the AIS scheme for compensating error in positional information.

We assume that the localization error in the GPS position of the FBS/MUE can be up to  $\pm 50\text{m}$ , and we study the effect on performance with the error values at 10m, 20m and 50m. Figure 5 plots the distribution of convergence of AIS for femto densities ( $\eta$ ) at 10% and 30%. As can be seen from the CDF results, the AIS scheme requires few additional iterations for convergence. This difference is accurately quantified by the KullbackLeibler divergence (KLD) with respect to no error. For femto densities  $\eta$  of 10%, we observe a maximum KLD of 39.4. As expected, the worst case KLD increases to 52.6 for  $\eta = 30\%$ . We see that for a 20% increase in  $\eta$ , the KLD increases by only 13.2. This small increase is because increase in  $\eta$  results in the requirements of more iterations for AIS

convergence across a larger number of FBSs.

## VI. CONCLUSION AND FUTURE WORK

This study describes the AIS mechanism for interference mitigation that relies on the estimation of femtocell interference for macrocell users based on geolocation information. Results based on simulations show that the AIS scheme is able to control femtocell power such that the number of macrocell users achieving target data rates increase by up to 158%, while resulting only 12.2% femtocell users receiving rates below the target. Further, the results show that the mechanism is able to work satisfactorily even with some level of inaccuracy in the location data. Future work is planned on improved AIS algorithms to reduce convergence time, and on extensions of the algorithm to OFDMA/4G systems.

### Acknowledgments

Research supported in part by US NSF grant #CMS-0626959

## REFERENCES

- [1] V. Chandrasekhar, J. Andrews, and A. Gatherer. "Femtocell networks: a survey". *Communications Magazine, IEEE*, 46(9):59–67, sep. 2008.
- [2] "Commercial cdma femtocells from airvana". <http://www.airvana.com/products/cdma-femtocell/>.
- [3] "Commercial cdma femtocells (ubicell) from samsung". <http://tinyurl.com/657tqjd>.
- [4] H.A. Mahmoud and I. Guvenc. "A comparative study of different deployment modes for femtocell networks". In *Personal, Indoor and Mobile Radio Communications, 2009 IEEE 20th International Symposium on*, pages 1–5, 2009.
- [5] D. Lopez-Perez, A. Valcarce, G. de la Roche, and Jie Zhang. "OFDMA femtocells: A roadmap on interference avoidance". *Communications Magazine, IEEE*, 47(9):41–48, sep. 2009.
- [6] V. Chandrasekhar and J. Andrews. "Uplink capacity and interference avoidance for two-tier femtocell networks". *Wireless Communications, IEEE Transactions on*, 8(7):3498–3509, jul. 2009.
- [7] H. Claussen. "Performance of macro- and co-channel femtocells in a hierarchical cell structure". In *Personal, Indoor and Mobile Radio Communications, 2007. PIMRC 2007. IEEE 18th International Symposium on*, pages 1–5, 2007.
- [8] L.T.W. Ho and H. Claussen. "Effects of user-deployed, co-channel femtocells on the call drop probability in a residential scenario". In *Personal, Indoor and Mobile Radio Communications, 2007. PIMRC 2007. IEEE 18th International Symposium on*, pages 1–5, 2007.
- [9] Femtoforum, "Interference management in OFDMA femtocells", whitepaper, mar. 2010 available at. [www.femtoforum.org/](http://www.femtoforum.org/).
- [10] Sundeeep Rangan. "Femto-macro cellular interference control with sub-band scheduling and interference cancelation". *CoRR*, abs/1007.0507, 2010.
- [11] V. Chandrasekhar, J.G. Andrews, T. Muharemovic, Zukang Shen, and A. Gatherer. "Power control in two-tier femtocell networks". *Wireless Communications, IEEE Transactions on*, 8(8):4316–4328, aug. 2009.
- [12] J. Espino and J. Markendahl. "Analysis of macro - femtocell interference and implications for spectrum allocation". In *Personal, Indoor and Mobile Radio Communications, 2009 IEEE 20th International Symposium on*, pages 2208–2212, 2009.
- [13] M.E. Sahin, I. Guvenc, Moo-Ryong Jeong, and H. Arslan. "Handling CCI and ICI in OFDMA femtocell networks through frequency scheduling". *Consumer Electronics, IEEE Transactions on*, 55(4):1936–1944, nov. 2009.
- [14] 3gpp2, cdma2000 high rate packet data air interface specification: Revision-2.0 (3gpp2 c.s0024). [http://www.3gpp2.org/public\\_html/specs](http://www.3gpp2.org/public_html/specs).
- [15] 3gpp tr 36.814 v9.0.0. [www.3gpp.org/ftp/Specs/archive/36\\_series/36.814/](http://www.3gpp.org/ftp/Specs/archive/36_series/36.814/).
- [16] G.J. Foschini and Z. Miljanic. "A simple distributed autonomous power control algorithm and its convergence". *Vehicular Technology, IEEE Transactions on*, 42(4):641–646, November 1993.